International Journal of Wireless Information Networks, Vol. 4, No. 2, 1997

A Novel EKF-Based Scheme for Tracking Code Delay Recovery in DS/CDMA Systems

Pilar Díaz[1,2] and Ramon Agustí[1]

Classical delay-lock loops (DLL) have been widely considered for code synchronization purposes in DS/CDMA systems, although they have not been devised for operation when channel fading is present. This paper describes a new code synchronization scheme based on a previously proposed extended Kalman filter (EKF) approach. The scheme proposed in this paper is able to operate under low signal-to-interference ratios (SIR), usual at the receiver input in cellular CDMA mobile environments, and it outperforms the behavior of previously proposed EKF-based schemes, which failed in such environments. Performance results under realistic mobile environment conditions are shown in terms of the mean time to lose lock (MTLL) and the tracking error variance σ_τ^2 for a wide range of SIR values and under Rayleigh multipath fading. Moreover, the Cramer–Rao lower boundon σ_τ^2 is also computed in order to validate the results obtained via simulations.

KEY WORDS: Extended Kalman filter; code synchronization; tracking; DS-CDMA.

1. INTRODUCTION

CDMA systems, claimed to be especially suited for working on a frequency-selective fading channel, have been widely treated in the literature in the recent years. Nevertheless, little effort has been devoted to the optimization of PN code delay recovering schemes required to correctly despread the DS spread-spectrum modulations in CDMA systems. In particular, the usually adopted code synchronizers are assumed to be based on DLL schemes, which are optimum in an AWGN channel, but not for operation in frequency-selective fading channels.

A first attempt to introduce specific synchronizers for operation in those environments was presented in Ref. 1, where an extended Kalman filter structure was proposed to jointly estimate the PN code delay in tracking and the channel impulse response. Nevertheless, this approach fails in the presence of the high-interference environments usual in mobile communication systems. For these cases, the MTLL takes a very low value because the signal-to-noise ratio (or signal-to-interfering power ratio) at the EKF input for realistic processing gains (such as 20 dB or even more) and for reasonable Eb/No ratios (about 5–10 dB) is so low that the deep channel fades prevent the EKF from acquiring synchronization.

In this paper a scheme based on the EKF approach is also proposed, but conveniently modified in order to improve its performance in terms of a larger MTLL figure and a smaller value of the mean root square error of estimation when operating under realistic conditions (i.e., signal-to-interference input ratios from −20 dB to 0 dB). In particular, the PN code delay and channel impulse response estimation are decoupled in this scheme, so the focus is put on the estimation of the PN code delay in the tracking phase. This means that an initial PN code misalignment lower than or equal to half a chip duration is assumed. The decoupled channel impulse response estimator is considered to be the usual suboptimum matched filtering approach with sampling

[1]Department of Signal Theory and Communications, UPC, Barcelona, Spain.

[2]Correspondence should be directed to Pilar Díaz, Department TSC, Campus Nord UPC, Mòdul D4, C/ Gran Capità s/n, 08034 Barcelona, Spain; e-mail: pilar@xaloc.upc.es.

1068-9605/97/0400-0089$12.50/0

times shifted by the actual PN code delay. The performance of this scheme is assessed by means of computer simulations in the presence of realistic propagation environments for band-limited Nyquist-filtering receivers.

The organization of this paper is as follows. In Section 2, the EKF theory is revised and the EKF-based scheme proposed for delay estimation as well as the complete system model are described in detail. Section 3 is devoted to dimension some system parameters and to evaluate, by means of the tracking error variance and the MTLL, the performance of the proposed scheme in a mobile environment under two different models of channel delay generation. Finally, in Section 4 some conclusions are drawn.

2. IMPROVED EKF FOR DELAY ESTIMATION IN CDMA ENVIRONMENTS

The combination of severe fading and large Doppler shifts arises usually in spread-spectrum communication channels. For this reason, demodulation in DS/CDMA systems cannot be accomplished without estimation of code delay. The specific problem of optimal synchronization in a direct-sequence spread-spectrum receiver is considered here as a specific application of the extended Kalman filter delay estimator.

2.1. The Extended Kalman Filter

The Kalman filter is basically a linear adaptive filter with feedback, and therefore it converges faster than other predictors. The extended Kalman filter (EKF) behaves similarly to a standard Kalman filter but for a nonlinear model. This model, if sufficiently smooth, can be approximated by a linear function by means of Taylor series. In Ref. 1 it is shown that the EKF is capable of estimating the channel delay in the tracking phase from the received samples and maintaining synchronization between the received code and the local code. Nevertheless, this delay estimator only works (i.e., the predictor only converges) when the signal-to-interfering ratio at the receiver input is large enough. Since this is not the usual condition in a CDMA cellular system, some signal processing before estimation is required.

For the sake of improving the signal-to-interfering power ratio at the EKF input, the delay estimator, proposed in this paper and shown in Fig. 1, consists of two blocks:

1. A first block known as "pre-filter," responsible for processing the received signal and improving the signal-to-interfering power ratio.
2. A second block, which is the EKF, now capable of estimating the channel delay in a CDMA environment. This is possible because the signal-to-interfering power ratio has been increased due to the processing performed by the previous block.

Let us focus on this second block, the EKF. The samples of the signal at its input, $X(k)$, can be expressed as follows:

$$X(k) = H(\tau(k)) + n(k) \tag{1}$$

where $H(\tau(k))$ are the samples of a nonlinear function of the delay $\tau(k)$, and $n(k)$ are the samples of a term representing interference and noise in general. The filter is able to compute the channel delay estimate every bit interval from these samples:

$$\hat{\tau}_{k/k} = E\{\tau(k) \mid X(k), X(k-1), \ldots, X(0)\} \tag{2}$$

The equations that rule the filter behavior, known as measurement-update equations, are given by [2]

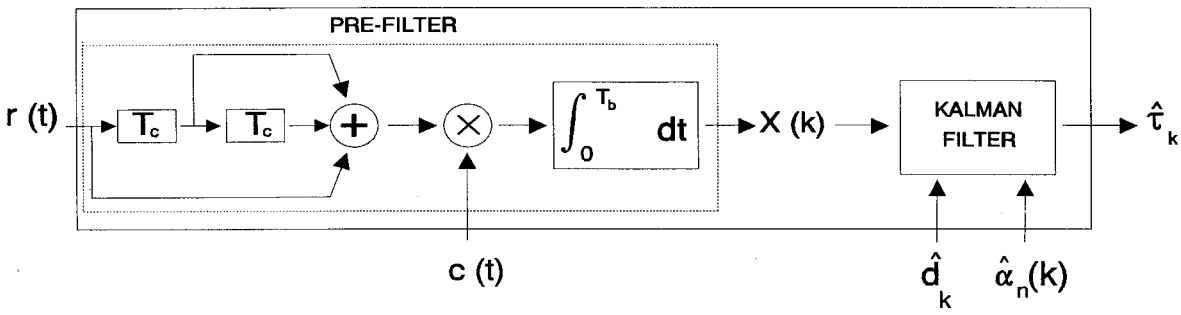

Fig. 1. Delay estimator based on the EKF.

$$\hat{\tau}_{k/k} = \hat{\tau}_{k/k-1} + K(k)[X(k) - H(\hat{\tau}_{k/k-1})]$$

$$K(k) = P_{k/k-1} \frac{\partial}{\partial \tau} H^*(\hat{\tau}_{k/k-1}) \cdot \left[\left| \frac{\partial}{\partial \tau} H(\hat{\tau}_{k/k-1}) \right|^2 P_{k/k-1} + \sigma_n^2 \right]^{-1}$$

$$P_{k/k} = \left[I - K(k) \frac{\partial}{\partial \tau} H(\hat{\tau}_{k/k-1}) \right] P_{k/k-1} \qquad (3)$$

where σ_n^2 is the variance of $n(k)$, and $K(k)$ and $P_{k/k}$ are known as the gain vector and the error covariance matrix, respectively. For the sake of simplicity, the channel delay is assumed to follow a first-order autorregressive (AR) process [1]:

$$\tau(k+1) = \gamma \tau(k) + w_\tau(k) \qquad (4)$$

where w_τ is a white Gaussian process with zero mean and variance σ_w^2, and γ is a parameter adjusted to account for transmitter and receiver timing jitter. According to the first-order AR model considered, the prediction equations, known as time-update equations, are given by

$$\hat{\tau}_{k+1/k} = \mathrm{Re}[\hat{\tau}_{k/k}]; \qquad P_{k+1/k} = P_{k/k} + \sigma_w^2 \qquad (5)$$

2.2. System Description

The complex envelope of the signal transmitted by a subscriber in a DS-CDMA system can be expressed as

$$s(t) = \sqrt{\frac{2S}{R_c(0)}} \sum_{k=-\infty}^{\infty} d_k c(t - kT_b) \qquad (6)$$

where T_b is the bit period, S the transmitted power, $R_c(0)$ the autocorrelation function of the spreading code $c(t)$ at the origin, and the binary symbol d_k represents the transmitted bit during the kth interval, as the signaling scheme considered for analysis in this paper is the coherent BPSK. The signal $c(t)$, which represents the spreading code assigned to a particular subscriber, is given by

$$c(t) = \sum_{i=0}^{N-1} c_i p(t - iT_c) \qquad (7)$$

where c_i are binary symbols, N is the number of chips/bit, and therefore the processing gain T_c is the chip period ($T_c = T_b/N$), and $p(t)$ is the pulse waveform of the code.

Supposethat $1/T_c$ is the bandwidth occupied by the real bandpass transmitted signal. The impulse response complex envelope of the time-variant frequency-selective channel can be modeled in this case as [3]

$$h_c(t, \tau') = \sum_{m=0}^{L-1} \alpha_m(t) \delta(\tau' - mT_c + \tau(t)) \qquad (8)$$

where L is the number of propagation paths and $\alpha_m(t)$ are their complex amplitudes. In a mobile environment, these amplitudes may be statistically characterized by a Gaussian complex distribution, and the mean received power of each path is determined by the power delay profile (PDP) of the channel.

From (6) and (8), the signal received can be expressed as

$$r(t) = \sum_{m=0}^{L-1} \alpha_m(t) s(t - mT_c + \tau(t)) + n_w(t) \qquad (9)$$

where $\tau(t)$ is the delay introduced by the mobile channel and $n_w(t)$ represents both interference from other users and thermal noise, although this noise may be neglected in an interference-limited cellular mobile environment.Later, for performance analysis purposes, $n_w(t)$ is assumed to be white Gaussian noise with null mean and variance σ_n^2.

From (1) it follows that the useful term $H(k)$ of the driving EKF signal $X(k)$ is only a function of $\tau(k)$, so the bit and the channel impulse response estimates have to be previously obtained in order to remove these variables from $H(\hat{\tau}_{k/k-1})$ in (3).

2.2.1. Bit Estimation

The bit estimation has been obtained from the conventional structure of a Rake receiver. Figure 2 illustrates the basic scheme of the receiver employed in this study.

Let τ_k be the delay introduced by the mobile channel during the kth bit interval, which will be assumed as nonvariant within this time interval, and $r_n(t)$ be a $(-nT_c)$-second delayed version of $r(t)$ ($n = 0, 1, 2$):

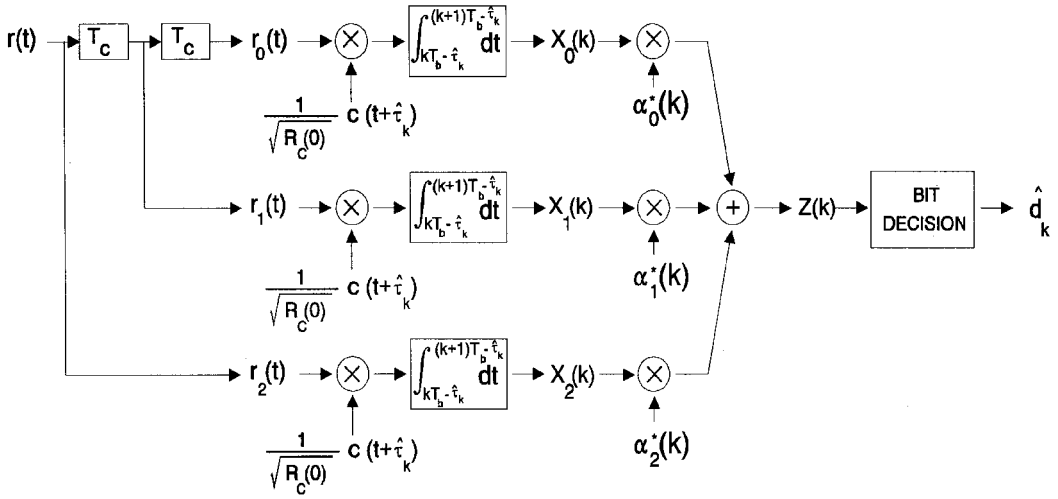

Fig. 2. Rake receiver with diversity $M = 3$.

$$r_n(t) = \sum_{m=0}^{L-1} \left(\sqrt{\frac{2S}{R_c(0)}}\, \alpha_m(t) \sum_{k=-\infty}^{\infty} \cdot d_k c(t-(m-n)T_c - kT_b + \tau(t)) \right) + n_w(t+nT_c) \tag{10}$$

The signal at the output of each delay unit is correlated with the code generated at reception, lined up with $c(t - kT_b + \tau_k)$ within this bit interval. If the term of interest is isolated into (10), i.e., $n = m$, then $r_n(t)$ may be expressed as

$$r_n(t) = \sqrt{2S/R_c(0)}\, \alpha_n(t) \sum_{k=-\infty}^{\infty} \cdot d_k c(t - kT_b + \tau_k) + n'(t+nT_c) \tag{11}$$

where the multipath has been included in the term which represents the interference noise produced by the other system users,

$$n'(t+nT_c) = \sum_{\substack{m=0 \\ m \neq n}}^{L-1} \left[\sqrt{\frac{2S}{R_c(0)}}\, \alpha_m(t) \sum_{k=-\infty}^{\infty} \cdot d_k c(t-(m-n)T_c - kT_b + \tau_k) + n_w(t+nT_c) \right] \tag{12}$$

Let $\hat{\tau}_k$ be the estimate of the channel delay and $\alpha_n(k)$ be the complex amplitude of the $n$thpropagation path during the kth bit interval. The signal at the output of each delay unit $r_n(t)$ is correlated with the code generated locally at reception, $c(t - kT_b + \hat{\tau}_k)$, in order to obtain the samples $X_n(k)$ $(n = 0, 1, 2)$ during this bit interval. These samples may be expressed as

$$\begin{aligned} X_n(k) &= \frac{1}{\sqrt{R_c(0)}} \int_{(k-1)T_b - \hat{\tau}_k}^{kT_b - \hat{\tau}_k} c(t - kT_b + \hat{\tau}_k) r_n(t)\, dt \\ &= \frac{\sqrt{2S}}{R_c(0)}\, d_k \alpha_n(k) \int_0^{T_b} c(t) c(t+e_k)\, dt \\ &\quad + n_n(k) \end{aligned} \tag{13}$$

where $e(k) = \tau(k) - \hat{\tau}(k)$ is the estimate error.

The term $n_n(k)$ in (13) is the interfering noise at the output of the nth correlator arm

$$n_n(k) = \frac{1}{\sqrt{R_c(0)}} \int_{(k-1)T_b - \hat{\tau}_b}^{kT_b - \hat{\tau}_b} \cdot c(t - kT_b + \hat{\tau}_k) n'(t+nT_c)\, dt \tag{14}$$

of zero mean and variance given by

$$\begin{aligned}\mathrm{Var}[n_n(k)] &= E\left[\int_0^{T_b}\int_0^{T_b}\frac{1}{R_c(0)}\,n'(t+nT_c+kT_b-\hat{\tau}_k)\right.\\ &\quad\left.\cdot\, n'(u+nT_c+kT_b-\hat{\tau}_k)c(t)c(u)\,dt\,du\right]\\ &= \frac{1}{R_c(0)}\int_0^{T_b}\int_0^{T_b}N_0\,\delta(t-u)c(t)c(u)\,dt\,du\\ &= N_0T_b \end{aligned}\tag{15}$$

Concerning the useful term of the signal $X_n(k)$, which will be designated as $H_n(k)$, let us note that it is a function of the autocorrelation of $c(t)$ and is given by

$$\begin{aligned}H_n(k) &= \frac{\sqrt{2S}}{R_c(0)}\,d_k\alpha_n(k)\int_0^{T_b}c(t)c(t+e_k)\,dt\\ &= \sqrt{2S}\,d_kT_b\alpha_n(k)\,\frac{R_c(\varepsilon)|_{\varepsilon=e_k}}{R_c(0)}\end{aligned}\tag{16}$$

where the expression for $R_c(\varepsilon)$ is

$$\begin{aligned}R_c(\varepsilon) &= \frac{1}{T_b}\int_{T_b}c(t)c(t+\varepsilon)\,dt\\ &= \frac{1}{T_b}\sum_i\sum_j c_ic_j\int_{T_b}\\ &\quad\cdot\, p(t-iT_c)p(t-jT_c+\varepsilon)\,dt\end{aligned}\tag{17}$$

If $R_p(\varepsilon)$ denotes the autocorrelation of the code waveform $p(t)$, then

$$R_c(\varepsilon) = \frac{1}{T_b}\sum_i\sum_j c_ic_jR_p(\varepsilon-(i-j)T_c)\tag{18}$$

Since the waveform approximately has a time duration equal to the chip interval, we should only retain in (18) those terms which are significant when $\varepsilon = e_k$ [see (17)]:

$$\begin{aligned}R_c(\varepsilon) &= \frac{1}{T_b}\sum_{i=0}^{N-1}\sum_{l=-Q}^{Q}c_ic_{i-l}R_p(\varepsilon-lT_c)\\ &= \frac{1}{T_b}\sum_{l=-Q}^{Q}R_p(\varepsilon-lT_c)\sum_{i=0}^{N-1}c_ic_{i-l}\end{aligned}\tag{19}$$

where Q is such that $R_p(e_k \pm QT_c) \simeq 0$. The second sum in (19) represents the sequence periodic correlation, which is given by

$$\begin{aligned}\theta_c(k) &= \sum_{i=0}^{N-1}c_ic_{i+k}\\ &= \begin{cases}N, & k \bmod N = 0\\ -1, & \text{otherwise}\end{cases}\end{aligned}\tag{20}$$

so one has

$$\begin{aligned}R_c(\varepsilon) &= \frac{1}{T_b}\left(NR_p(\varepsilon)-\sum_{\substack{|l|<Q\\ l\neq 0}}R_p(\varepsilon-lT_c)\right)\\ &= \frac{1}{T_c}\left(R_p(\varepsilon)-\frac{1}{N}\sum_{\substack{|l|<Q\\ l\neq 0}}R_p(\varepsilon-lT_c)\right)\end{aligned}\tag{21}$$

When this is computed for $\varepsilon = 0$, the following expression is obtained:

$$R_c(0) = \frac{1}{T_c}\left(R_p(0)-\frac{1}{N}\sum_{\substack{|l|<Q\\ l\neq 0}}R_p(lT_c)\right)\tag{22}$$

Finally, the sample value at the decision unit input

$Z(k)$ (see Fig. 2) is given by

$$Z(k) = \sum_{n=0}^{M-1} \hat{\alpha}_n^*(k) X_n(k)$$

$$= \sum_{n=0}^{M-1} \hat{\alpha}_n^*(k)[H_n(k) + n_n(k)] \tag{23}$$

where M is the number of Rake arms. If (16) is replaced in the above expression, we obtain

$$Z(k) = \sum_{n=0}^{M-1} \hat{\alpha}_n^*(k) \cdot \left(\sqrt{2S}\, d_k T_b \alpha_n(k) \frac{R_c(\varepsilon)|_{\varepsilon=e_k}}{R_c(0)} + n_n(k) \right)$$

$$= d_k \sqrt{2S}\, T_b \frac{R_c(\varepsilon)|_{\varepsilon=e_k}}{R_c(0)} \cdot \sum_{n=0}^{M-1} \hat{\alpha}_n^*(k)\alpha_n(k) + \sum_{n=0}^{M-1} \hat{\alpha}_n^*(k) n_n(k) \tag{24}$$

where $\hat{\alpha}_n(k)$ is the channel amplitude estimate.

Since coherent BPSK is the signaling scheme considered in this study, the bit estimate at the decision unit output is $\hat{d}_k = \text{sign}[\text{Real}(Z(k))]$.

2.2.2. Impulse Response Estimation

Let us see how to compute the estimate of the channel impulse response with a filter matched to the pseudorandom sequence in a DS/CDMA system. Although this technique is not optimal in the sense that sequences are not ideally orthogonal [4], we will adopt this simple estimation technique since it could be appropriate for a CDMA environment. Anyway, it is considered as a first approach to assess the performance of the EKF-based structure proposed in this paper as a PN code delay recovering scheme.

Let us assume that a PN sequence without modulation is being transmitted and let α_j be the impulse response of the channel and $pn(j)$ the PN sequence. The samples of the received signal at the matched filter input in the absence of interchip interference can be expressed as

$$x(j) = \sum_{l=0}^{L-1} \alpha_l pn(j-l) \tag{25}$$

Let $c(j)$ be the impulse response of the matched filter, which is given by

$$c(j) = pn(N-j) \tag{26}$$

When the thermal noise is negligible with regard to the interference power, the signal $y(j)$ at the filter output takes the following form:

$$y(j) = x(j) * c(j) = \sum_{i=0}^{N-1} \sum_{l=0}^{L-1} \alpha_l pn(i-l) c(j-i) \simeq N\alpha_j \tag{27}$$

From (27) it can be seen that the samples obtained at the output of the matched filter every T_c seconds are sufficient to get the estimate of the channel amplitudes $\hat{\alpha}_j$.

2.3. The Proposed EKF-Based Scheme for Delay Estimation

After establishing a procedure to estimate the transmitted bit and the channel impulse response, let us analyze the channel delay estimation scheme based on the EKF for operation in tracking. The implementation of such a delay estimator is illustrated in Fig. 1. The samples at the EKF input are given by

$$X(k) = \sum_{n=0}^{M-1} \int_{(k-1)T_b}^{kT_b} c(t - kT_b) r(t + nT_c)\, dt$$

$$= \sum_{n=0}^{M-1} \sqrt{2S}\, d_k T_b \alpha_n(k) \frac{R_c(\varepsilon)|_{\varepsilon=\tau_k}}{R_c(0)} + \sum_{n=0}^{M-1} n_n(k) \tag{28}$$

Let us note from Figs. 1 and 2 that the local codes in both structures (the Rake receiver and the delay estimator) are delayed $\hat{\tau}_k$ seconds. The equilibrium point of the filter ($\hat{\tau}_k \rightarrow \tau_k$) should be prevented from being near the origin area ($\hat{\tau}_k \rightarrow 0$) in order to have a correct operation of the synchronism scheme. The reason for this fact is that the gain vector $K(k)$, which is proportional to the derivative of $R_c(\tau)$, is zero in the absence of noise, or not defined in this area, depending on the pulse waveform employed. Therefore, if the gain vector $K(k)$ were zero, the filter would not be able to follow

the variations of the delay even if $[X(k) - \hat{H}(k)]$ was not near zero, as the measurement-update equation, given by $\hat{\tau}_k = \hat{\tau}_{k-1} + K(k)[X(k) - \hat{H}(k)]$, shows.

To avoid the origin area ($\hat{\tau}_k \rightarrow 0$), a control subroutine has been designed in order to force the filter to work in what will be known as the "optimum working area." The proposed algorithm consists in having a "slightly misalignment" between the received code and the local code at the receiver. Whenever the estimate of τ_k takes an absolute value lower than a given threshold, e.g., $0.2T_c$, the local code generated at the receiver is shifted in order to increase τ_k and prevent the filter from working around the origin area. Whenever the estimate of τ_k takes an absolute value greater than another given threshold, e.g., $0.4T_c$, the local code is shifted toward the other direction to ensure that the filter is in tracking, i.e., to ensure both codes are not misaligned more than half a chip.

Moreover, it is necessary to dimension the initial values of the filter. The equations that rule the filter behavior are described in (3), so the measurement-update equation concerning the channel delay estimate is given by $\hat{\tau}_k = \hat{\tau}_{k-1} + K(k)[X(k) - \hat{H}(k)]$, where the samples $X(k)$

$$X(k) = H(k) + \sum_{n=0}^{M-1} n_n(k) \tag{29}$$

are formulated in (28).

Since the term of interest of the samples at the EKFinput, $H(k)$ is an even function with respect to the channel delay τ_k, the filter has two different equilibrium points:

$$H(k)\big|_{\varepsilon=\tau_k} = \sum_{n=0}^{M-1} \sqrt{2S}\, d_k T_b \alpha_n(k)\, \frac{R_c(\varepsilon)\big|_{\varepsilon=\tau_k}}{R_c(0)} = H(k)\big|_{\varepsilon=-\tau_k} \tag{30}$$

given that an autocorrelation function like $R_c(\varepsilon)$ is always an even function when the value of $\hat{\tau}_{-1}$ is set at the first filter iteration ($k = 0$). Therefore, it happens that if $\hat{\tau}_{-1}$ is initially set to the correct sign, the filter will converge to the correct equilibrium point ($\hat{\tau}_k \rightarrow \tau_k$), but if it is initially set to the opposite sign, the filter will reach the other equilibrium point ($\hat{\tau}_k \rightarrow -\tau_k$) and will become stable since

$$X(k)\big|_{\tau=\tau_k} - \hat{H}(k)\big|_{\tau=-\tau_k} \rightarrow 0 \tag{31}$$

In order to solve this problem of initialization, we propose to introduce a block that computes a signal comparison, as follows. If we consider no noise, when the filter has been initially set to the correct sign and $\hat{\tau}_k \rightarrow \tau_k$, the sample $X(k)$ at the EKF input (see Fig. 1)

$$X(k) = \sum_{n=0}^{M-1} \sqrt{2S}\, d_k T_b \alpha_n(k)\, \frac{R_c(\varepsilon)\big|_{\varepsilon=\tau_k}}{R_c(0)} \tag{32}$$

is smaller than the sum of the samples $X_n(k)$ ($n = 0, 1, 2$) at the Rake correlator output (see Fig. 2):

$$\sum_{n=0}^{M-1} X_n(k) = \sum_{n=0}^{M-1} \sqrt{2S}\, d_k T_b \alpha_n(k)\, \frac{R_c(\varepsilon)\big|_{\varepsilon=\tau_k-\hat{\tau}_k}}{R_c(0)} \simeq \sum_{n=0}^{M-1} \sqrt{2S}\, d_k T_b \alpha_n(k) \tag{33}$$

Otherwise, when it is initially set to the incorrect sign and $\hat{\tau}_k \rightarrow -\tau_k$, the sample $X(k)$ at the EKF input

$$X(k) = \sum_{n=0}^{M-1} \sqrt{2S}\, d_k T_b \alpha_n(k)\, \frac{R_c(\varepsilon)\big|_{\varepsilon=\tau_k}}{R_c(0)} \tag{34}$$

is larger than the sum of the samples $X_n(k)$ ($n = 0, 1, 2$), which in this case is given by the following expression:

$$\sum_{n=0}^{M-1} X_n(k) = \sum_{n=0}^{M-1} \sqrt{2S}\, d_k T_b \alpha_n(k)\, \frac{R_c(\varepsilon)\big|_{\varepsilon=\tau_k-\hat{\tau}_k}}{R_c(0)} \simeq \sum_{n=0}^{M-1} \sqrt{2S}\, d_k T_b \alpha_n(k)\, \frac{R_c(\varepsilon)\big|_{\varepsilon=2\tau_k}}{R_c(0)} \tag{35}$$

A signal comparison will allow us to find out if the filter has been initially set to the right sign. Otherwise, the filter should be again initialized with the opposite sign.

In practice, when the signal is corrupted with noise, the procedure described above can be repeated during several bits in order to filter a certain amount of noise

and increase the reliability on detecting the correctness of the sign. This iteration procedure has been employed in the simulations carried out to assess the delay estimator performance, which will be presented in the next section.

In summary, the scheme proposed here to perform the channel delay estimate for DS-CDMA systems under multipath fading is the structure shown in Fig. 1. The control subroutine proposed in order to achieve an optimum operation can be summarized as:

1. Set the filter parameters and check the estimate sign with a signal comparison:

$$\sum_{n=0}^{M-1} X_n(k) > X(k) \tag{36}$$

2. If the sign is incorrect, set the parameters to the opposite sign. Otherwise, check regularly the filter working area to ensure that

$$0.2T_c < \hat{\tau}_k < 0.4T_c \tag{37}$$

3. ESTIMATOR PERFORMANCE IN MOBILE ENVIRONMENTS

To analyze the performance of the channel delay estimator, the whole receiver has been simulated under realistic mobile environment conditions, which have been selected for the purpose of evaluation. To do this, the classical Doppler spectrum [5] has been assumed with a Doppler frequency value of 50 Hz, which accounts for a mobile speed of 60 km/h and a carrier frequency of 900 MHz. The channel PDP has been modeled as exponential because of its wide acceptance [6] and the delay spread normalized to the bit interval has been set to $D_{\text{sn}} = 0.01$. The signaling scheme considered is the coherent BPSK at a bit rate of $R_b = 10$ Kbps and the length of the maximum-length shift register sequences employed in the simulations is assumed to be $N = 127$, which also represents the processing gain. Therefore, the signal-to-interference ratio at the receiver input may be expressed as

$$\text{SIR} = (E_b/N_0)/N \tag{38}$$

The AR parameter in Eq. (4) for $\tau(k)$ was set in the EKF to correspond to the case of nearly constant delay, so γ was taken to be equal to 0.9999.

The pulse waveforms considered in the design and analysis of the synchronism scheme proposed in this paper are the Nyquist pulses with rolloff zero. Let us thus obtain the function $R_c(\varepsilon)$ in terms of the autocorrelation function of a Nyquist pulse $R_p(\varepsilon)$:

$$\frac{R_c(\varepsilon)}{R_c(0)} = \frac{T_c}{T_b}\left(NR_p(\varepsilon) - \sum_{\substack{k=-Q \\ |k|\neq 0}}^{Q} R_p(\varepsilon - kT_c)\right)$$

$$= R_p(\varepsilon) - \frac{1}{N}\sum_{\substack{k=-Q \\ |k|\neq 0}}^{Q} R_p(\varepsilon - kT_c) \tag{39}$$

where

$$R_p(\varepsilon) = \text{sinc}(\varepsilon/T_c)$$
$$R_c(0) = R_p(0)/T_c = 1/T_c \tag{40}$$

Concerning the channel impulse response, a data frame has been designed for simulation purposes in order to estimate this response during the reception of a known preamble, composed of Q bits, and estimate the transmitted bits during the reception of the information block, composed of D bits. To have better performance in a time-variant environment, the estimates of the channel amplitudes are updated during the reception of the information block according to a data-aided procedure. Q and D have been dimensioned in the simulation to 5 and 95 bits, respectively, since they are suitable values for Doppler shifts around 50 Hz and for high frame efficiencies. By using this procedure instead of a continuous pilot broadcasted by the base station in the downlink, either the uplink or the downlink paths may be considered in the analysis.

3.1. First-Order AR Model Parameters

To undertake the filter design, the first step was the computation of typical values of the variance σ_w^2 of the white Gaussian process $w_\tau(k)$, which represents the first-order AR model. To do this, let us note that the delay variation between two consecutive bits is given by $\Delta\tau = \Delta e/c = vT_b/c$ if the mobile speed v is assumed to be constant within this interval. Here Δe is the distance covered by the mobile within this time interval and $c = 3 \times 10^8$ is the light speed.

Table I. Delay Shift as a Function of the Mobile Speed

v (m/s)	$\Delta\tau/T_c$
1.	4.2×10^{-7}
5.	2.1×10^{-6}
10.	4.2×10^{-6}
50.	2.1×10^{-5}

Table I shows the channel delay shifts normalized to the chip period T_c as a function of the mobile speed for $R_b = 10$ Kbps and $N = 127$. In any of these cases, the delay shifts are much smaller than the chip period. This is reasonable because otherwise it would not be possible to follow the channel delay variations. The values included in Table I are similar to the time shifts produced by system clock drifts.

Simulation results for different values of σ_w showed that the EKF converged quickly in tens of iterations for SIR $= -15$ dB when $\sigma_w = 1.27 \times 10^{-4}\ T_c$ and $\sigma_w = 1.27 \times 10^{-5}\ T_c$ [7]. For $\sigma_w = 1.27 \times 10^{-6}\ T_c$, the filter evolution was much slower, which resulted in a very long "pull-in" time. The parameter σ_w was assumed to be known by the filter, i.e., the value employed to compute the channel delay estimate in the EKF, which is referred to as σ'_w, was the same as the value used for generating the actual delay introduced by the channel σ_w according to the first-order AR model.

Another parameter of quality is the normalized estimate error jitter σ_τ^2, which quantifies the delay estimate tightness and is defined as $\sigma_\tau^2 = E[(\tau(k) - \hat{\tau}(k|k-1))^2/T_c^2]$.

Figure 3a shows the error jitter as a function of σ_w or σ'_w for the range from $1.27 \times 10^{-6}\ T_c$ to $1.27 \times 10^{-3}\ T_c$, and for SIR $= -15$ dB. The synchronizer is able to work for values of σ_w smaller than (or equal to) $1.27 \times 10^{-4}\ T_c$, but for larger values the jitter increases very quickly, which results in performance degradations. This is why, from a design point of view, σ'_w has been set to $1.27 \times 10^{-5}\ T_c$. The value $\sigma_w = 1.27 \times 10^{-4}\ T_c$ was not chosen because it was on the limit of the range of convergence. To check the validity of such a selection, the error jitter for different σ_w was computed while keeping constant $\sigma_w = 1.27 \times 10^{-5}\ T_c$ as a design parameter. The results, illustrated in Fig. 3b, show that the choice is correct, since the filter even converges for variance values greater than $\sigma_w = 1.27 \times 10^{-5}\ T_c$.

Finally, and in order to validate somehow the results obtained, we resorted to the Cramer–Rao bound [8]. When the delay, though unknown, is deterministic (i.e., it does not change in time), the tracking error variance for any unbiased estimator is lower bounded by the Cramer–Rao bound, which for delay estimation is given by [1]

$$E\{[\hat{\tau} - \tau]^2\} \geq \sigma_n^2/2 \sum_{k=1}^{K} \left| \frac{\partial}{\partial \tau} X^*(k) \right|^2 \qquad (41)$$

where K is the whole number of samples upon which the estimate is based.

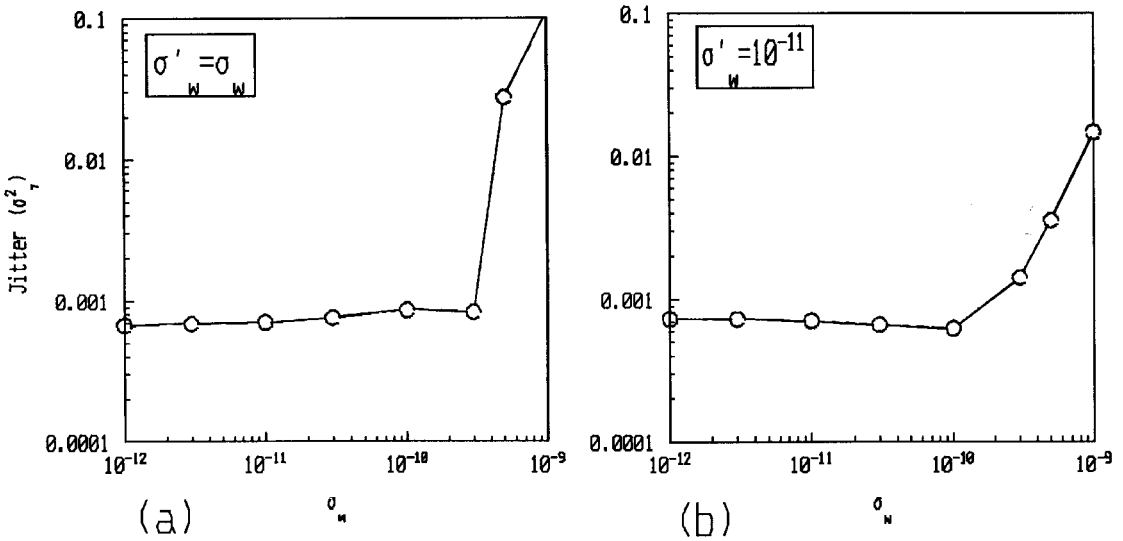

Fig. 3. Normalized delay estimate jitter as a function of the parameter σ_w of the first-order AR model (SIR $= -15$ dB).

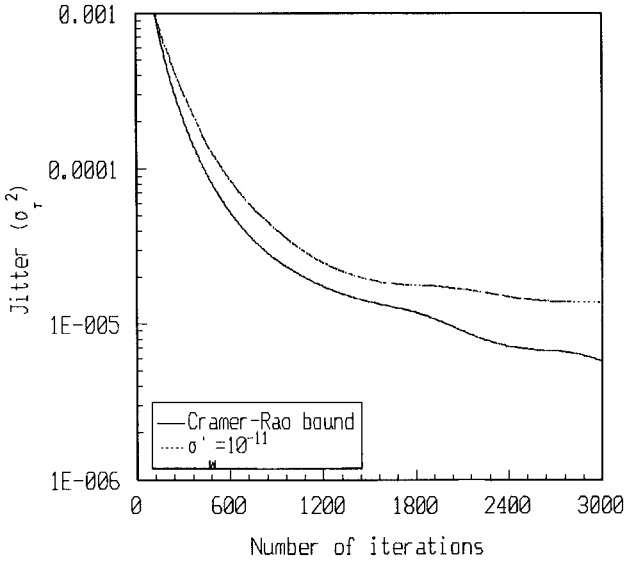

Fig. 4. Cramer–Raobound.

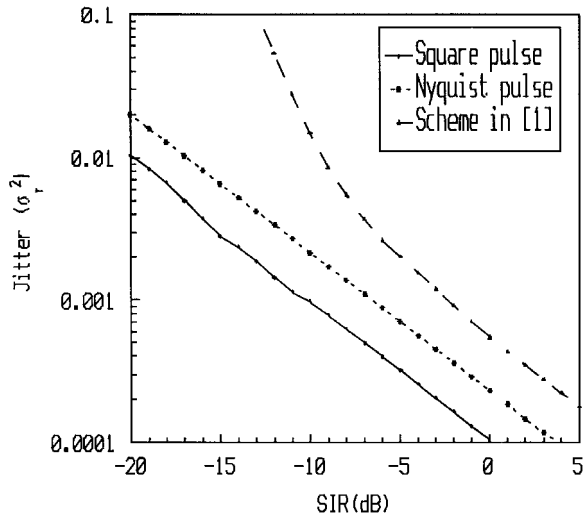

Fig. 5. Normalized delay estimate jitter as a function of SIR (dB) for the scheme proposed in Ref. 1 and for rectangular and Nyquist pulses with the enhanced scheme.

In Fig. 4, the performance of the EKF-based synchronism scheme is compared to the Cramer–Rao bound. Results shown in this figure demonstrate how the estimator proposed in this paper is very close to the optimum. If the design parameter σ'_w had been set to a smaller value, the results obtained would have been even closer to the Cramer–Rao bound, as it is assumed to be a first-order AR process in the estimation process, whereas the actual delay, though unknown, is a constant.

3.2. System Performance: Jitter and Mean Time to Lose Lock (MTLL)

To assess the performance of an estimator, it is also necessary to evaluate the jitter as a function of the SIR at the receiver input and the MTLL of the estimator. The MTLL is defined as the mean time in which the filter is able to maintain the system synchronism.

Although the pulse waveforms considered in the analysis are the Nyquist pulses, in order to get some knowledge of the influence of the waveforms on the delay estimator performance, square pulses have been also introduced, under identical channel conditions, as an example for comparison purposes. Figure 5 shows the normalized jitter for rectangular and Nyquist pulses for the scheme proposed in this paper. The values obtained show that the rms jitter is lower than the 10% of the chip interval T_c even for SIR $= -20$ dB. For comparison purposes, results for the scheme proposed in Ref. 1 have also been included, which have been obtained with perfect bit and channel estimates under the same environment assumptions.

To evaluate the MTLL, long simulations have been run in order to allow the evolution of the estimator within a period equivalent to 1 h of operation or until the error reaches values greater than half a chip. We have analyzed the behavior of both the structure proposed in Ref. 1 and the enhanced scheme proposed in this paper for code synchronization. The results obtained from these simulations are depicted in Fig. 6 as a function of the SIR ratio. Results on the MTLL for a linear model, which will be introduced in the next section, are also illustrated. This figure shows that the EKF-based scheme is able to maintain code synchronization even for very low SIR ratios. It is also illustrates the poor behavior of the EKF approach presented in Ref. 1, at least for those SIR ratios which are common in DS/CDMA cellular systems. If the results obtained for the enhanced EKF-based scheme are also compared to those obtained in classical DLL-based approaches, an important improvement of the performance offered by the EKF-based estimator is obtained. For a DLL-based synchronism scheme of a CDMA system working at $R_b = 10$ Kbps, the MTLL obtained in Ref. 9 for a VCO stability of 10^{-5} and a processing gain of 20 dB was approximately 20 s. The mobile channel was modeled by two independent Rayleigh propagation paths with an SIR $= -15$ dB for the first one and an SIR $= -25$ dB for the second one and for Doppler shifts of 50 Hz.

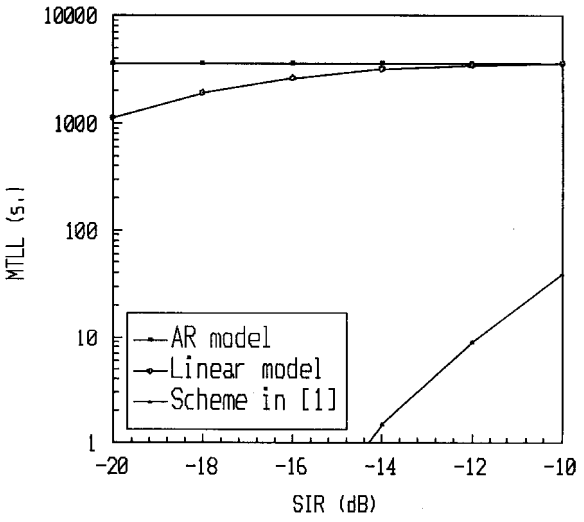

Fig. 6. MTTL as a function of SIR (dB) for the first-order AR model with both the scheme proposed in Ref. 1 and the enhanced scheme and for the linear model ($v = 30$ m/s).

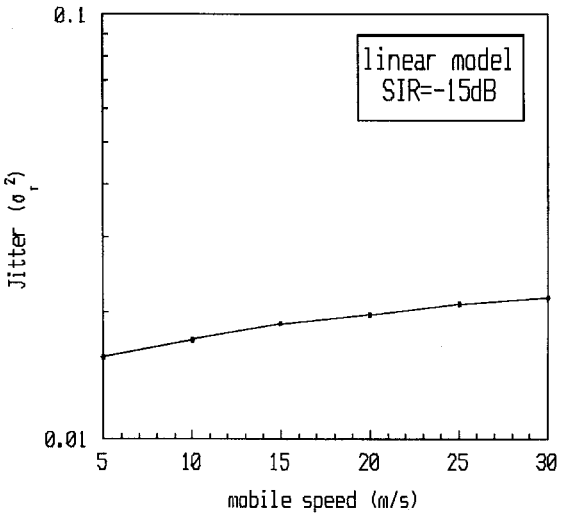

Fig. 7. Normalized delay estimate jitter as a function of the mobile speed v (m/s) for SIR $= -15$ dB.

In the case analyzed in this section, it has been assumed that the filter perfectly knows the delay generation model of the real channel, i.e., the first-order AR process. This might not happen in practice, so the filter behavior when the real delay generation model is not the same as the AR process considered in the EKF will be analyzed in the next section.

3.3. Linear Model for Delay Generation

In order to check the validity of the EKF-based synchronism scheme proposed in this paper, a linear model for generation of the real channel delay will be introduced. Such a model is useful for checking the filter robustness, as it consists in the assumption of a constant increase (or decrease) of the channel delay, which will be dependent on the mobile speed. By doing this, it is intended to model a mobile coming near or going away from the base station at a constant speed. Consequently, the delay introduced by the channel varies from interval to interval according to the expression $\tau(k+1) = \tau(k) + \Delta\tau$, where the delay increment is $\Delta\tau = vT_b/c$, with c the light speed and v the mobile speed.

Independently of how the channel delay is actually generated, the EKF algorithm is designed assuming a first-order AR model [see (4)] for two reasons: for its simplicity and because in practice the real model of the channel variation is not known since it is dependent on the mobile, the environment, and other factors. The analysis shown in this section intends to prove that even in this case the filter is still able to compute a high-quality estimate.

For the sake of assessing the system performance in this case, we have obtained the jitter at the estimator output as a function of the mobile speed v. Figure 7 depicts the results obtained for an SIR equal to -15 dB. From this figure, we can conclude that the EKF-based synchronism scheme proposed in this paper is capable of recovering the delay introduced by the channel with the little error, even when the generation model assumed by the EKF is different from the real one. Results for other models (random models) are shown in Ref. 7.

Results showing the MTLL are illustrated in Fig. 6. They prove that the EKF-based synchronism scheme proposed in this paper does not diverge within a period of time long enough and within the range of low SIR ratios considered. Therefore, it is a suitable scheme for code synchronization in a DS/CDMA system in the presence of Rayleigh multipath fading, or even for synchronization among the different users at the base station in DS/CDMA synchronous systems, as shown in Ref. 10.

4. CONCLUSIONS

In this paper, a novel delay recovering scheme based on the extended Kalman filter (EKF) has been proposed to operate in the tracking phase. It has been demonstrated that it works properly in fading multipath environments, even for extremely low SIR, thanks to

the preprocessing performed before the adaptive filter, and without the need to estimate the number of propagation paths arriving at the receiver. The preprocessing performed on the received signal before being fed to the EKF makes necessary the use of a control subroutine such as that described in the paper.

The delay generation model assumed by the filter algorithm is a first-order AR model with parameter σ_w'. It has also been shown that even in the case that the real model does not coincide with that assumed by the EKF, the delay channel estimator performance is good enough. Moreover, the filter parameters have been dimensioned for optimum operation and it has been shown that the proposed scheme presents good performances in terms of the normalized delay estimate jitter and MTLL.

REFERENCES

1. R. A. Iltis, Joint estimation of PN code delay and multipath using the extended Kalman filter, *IEEE Transactions on Communications*, Vol. 38, No. 10, pp. 1677–1685, 1990.
2. B. D. O. Anderson and J. B. Moore, *Optimal Filtering*, Prentice-Hall, Englewood Cliffs, New Jersey, 1979.
3. J. G. Proakis, *Digital Communications*, McGraw-Hill, New York, 1989.
4. A. P. Clark, Z. C. Zhu, and J. K. Joshi, Fast start-up channel estimation, *IEE Proceedings*, Vol. 131, Part F, No. 4, pp. 375–382, 1984.
5. W. C. Jakes, *Microwave Mobile Communications*, Wiley, New York, 1974.
6. J. C. Bultitude, S. A. Mahmoud, and W. A. Sullivan, A comparison of indoor radio propagation characteristics at 910 MHz and 1.75 GHz, *IEEE Journal on Selected Areas in Communications*, Vol. 7, No. 1, pp. 20–30, 1989.
7. P. Díaz and R. Agustí, Analysis of a PN code delay estimator using the extended Kalman filter in a CDMA cellular system. In *Proceedings of Wireless'93*, Calgary, pp. 279–284, 1993.
8. J. M. Mendel, *Lessons in Digital Estimation Theory*, Prentice-Hall, Englewood Cliffs, New Jersey, 1987.
9. J. J. Olmos and R. Agustí, Performance analysis of a second order delay-lock loop with application to a CDMA system with multipath propagation. In *Proceedings of ICUPC'92*, Dallas, pp. 209–213, 1992.
10. P. Díaz and R. Agustí, Performance of a linear interference canceller for a DS/CDMA synchronous system based on the EKF delay estimator. In *Proceedings of VTC'95*, Chicago, pp. 68–71, 1995.

Pilar Díaz (M'94) was born in Barcelona, Spain, on November 29, 1967. She received the Engineer and Doctor Engineer degrees in telecommunication engineering from the Universitat Politècnica de Catalunya (UPC), Spain, in 1990 and 1994, respectively. In 1990, she joined the Escola Tècnica Superior d'Enginyers de Telecomunicació de Barcelona, Spain, where she became an Assistant Professor in 1991 and a Associate Professor in 1995. She has been working in the field of digital radio communications with particular emphasis on personal, indoor, and mobile communications. Her main research interests lie in the area of radio multiple access and spread-spectrum systems, both FH and DS/CDMA systems. She participated in the RACE Program and Cost European Action, and at present she is actively participating in the ACTS European Research Program.

Ramón Agustí (M'78) was born in Riba-roja d'Ebre, Spain, on August 15, 1951. He received the Engineer of Telecommunication degree from the Universidad Politécnica de Madrid, Spain, in 1973, and the Ph.D. degree from the Universitat Politècnica de Catalunya, Spain, 1978. In 1973, he joined the Escola Tècnica Superior d'Enginyers de Telecomunicació de Barcelona, Spain, where he became Full Professor in 1987. He has been working in the field of digital communications with particular emphasis on digital radio, both fixed radio relay and mobile communications. He has also been concerned with the performance analysis and development of frequency-hopped spread-spectrum systems. He participated in the COST 231 and RACE European research programs and currently is participating in the ACTS program. His research interests are in the area of mobile communications with special emphasis on CDMA systems and packet radio networks.